JACS
JOURNAL OF THE AMERICAN CHEMICAL SOCIETY

ARTICLE

pubs.acs.org/JACS

A Stable Aminothioketyl Radical in the Gas Phase

Magdalena Zimnicka,[†] Joshua A. Gregersen, and František Tureček*

Department of Chemistry, University of Washington, Bagley Hall, Box 351700, Seattle, Washington 981195-1700, United States

Supporting Information

ABSTRACT: We report the first preparation of a stable aminothioketyl radical, $CH_3C^{\bullet}(SH)NHCH_3$ (**1**), by fast electron transfer to protonated thioacetamide in the gas phase. The radical was characterized by neutralization−reionization mass spectrometry and ab initio calculations at high levels of theory. The unimolecular dissociations of **1** were elucidated with deuterium-labeled radicals $CH_3C^{\bullet}(SD)NHCH_3$ (**1a**), $CH_3C^{\bullet}(SH)NDCH_3$ (**1b**), $CH_3C^{\bullet}(SH)NHCD_3$ (**1c**), and $CD_3C^{\bullet}(SH)NHCH_3$ (**1d**). The main dissociations of **1** were a highly specific loss of the thiol H atom and a specific loss of the N-methyl group, which were competitive on the potential energy surface of the ground electronic state of the radical. RRKM calculations on the CCSD(T)/aug-cc-pVTZ potential energy surface indicated that the cleavage of the S−H bond in **1** dominated at low internal energies, $E_{int} < 232$ kJ mol^{-1}. The cleavage of the N−CH_3 bond was calculated to prevail at higher internal energies. Loss of the thiol hydrogen atom can be further enhanced by dissociations originating from the B excited state of **1** when accessed by vertical electron transfer. Hydrogen atom addition to the thioamide sulfur atom is calculated to have an extremely low activation energy that may enable the thioamide group to function as a hydrogen atom trap in peptide radicals. The electronic properties and reactivity of the simple aminothioketyl radical reported here may be extrapolated and applied to elucidate the chemistry of thioxopeptide radicals and cation radicals of interest to protein structure studies.

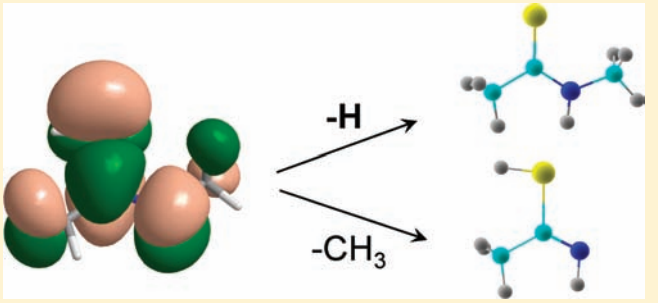

INTRODUCTION

Aminoketyl and aminothioketyl radicals, R−C$^{\bullet}$(XH)−NH−R′, where X = O or S, are transient organic species that are formed by radical additions to amide or thioamide groups. When present in biomolecules, amide radicals appear as reactive intermediates of DNA and RNA damage due to redox and radical reactions involving cytosine and uracil nucleobases, respectively.[1,2] Aminoketyl radicals have also been suggested as crucial reactive intermediates in dissociations of peptide and protein cation radicals formed by protonation followed by electron attachment.[3] Such hydrogen-rich cation-radicals[4a] are important in mass spectrometric analysis for protein sequencing that is based on ion-electron recombination.[4b] A few simple aminoketyl radicals, for example, $HC^{\bullet}(OH)NH_2$,[5a] $CH_3C^{\bullet}(OH)NH_2$,[5b] and $CH_3C^{\bullet}(OH)NHCH_3$,[5c,d] have been generated and studied in the gas phase. A particular feature of aminoketyl radical chemistry is the competing unimolecular dissociations involving the O−H and N−C bonds.[5c] When occurring in a peptide cation-radical, an O−H bond dissociation results in the loss of a hydrogen atom, whereas N−C_α bond dissociations form sequence-specific backbone fragments. The N−C_α bond dissociations have been shown by experiment[6] and theory[7] to depend on the cation-radical conformation, which is related to the conformation of the precursor peptide ion.

Thioxopeptides represent peptide derivatives in which one or more carbonyl oxygens have been replaced by sulfur. A direct conversion of amides to thioamides can be accomplished by the reaction with Lawesson's reagent[8−10] and related species.[11−14] The presence of a thioamide group in the peptide backbone results in several structural changes. The energy barrier for a rotation about the CS−NH bond is 8−12 kJ mol^{-1} higher than that for the CO−NH bond, due to the more pronounced double-bond character of the thioxopeptide C−N bond.[15] The typical C═S double bond (1.64 Å) is longer than the C═O bond (1.24 Å).[16,17] The larger covalent[18] and van der Waals radii[19] of sulfur restrict the allowable φ, ψ-angles in the vicinity of thioxo peptide groups.[20] These structure modifications introduced by thioamide substitution in peptides have been utilized to study peptide and protein secondary structure and biological activity.[20−23]

Despite the utility of thioamides for studying the effects of oxygen−sulfur substitution in peptides, peptide radicals and cation-radicals in which one or more amide groups have been replaced by thioamide groups have not been investigated so far, and thus the properties of aminothioketyl radicals representing hydrogen-rich thioamide radicals are unknown. Here, we report the first preparation of an aminothioketyl radical in the gas phase. We chose the hydrogen atom adduct to *N*-methylthioacetamide, $CH_3C^{\bullet}(SH)NHCH_3$ (**1**), which is a simple model mimicking a hydrogen-atom adduct to the thioamide group in a thioxopeptide. Radical **1** and its deuterium-labeled derivatives **1a**−**1d**

Received: April 19, 2011
Published: May 26, 2011

Scheme 1

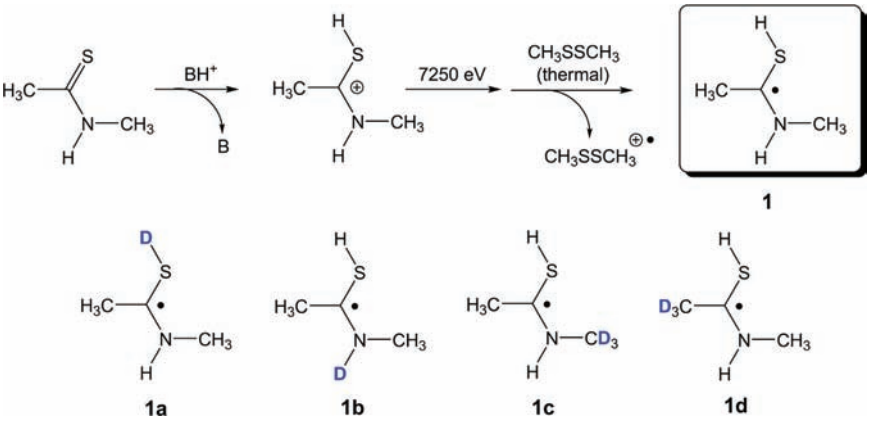

(Scheme 1) are generated from the corresponding cations by femtosecond electron transfer from a polarizable electron donor and investigated using neutralization−reionization mass spectrometry ($^{+}$NR^{+}MS).[24,25] The observed dissociation pathways are studied by high-level ab initio calculations. Additionally, Rice−Ramsperger−Kassel−Marcus (RRKM) calculations of unimolecular rate constants are performed to assess the dissociation kinetics. The results obtained for radical **1** are compared to those obtained previously for another standard peptide model, the 1-hydroxy-1-(*N*-methyl)aminoethyl radical, $CH_3C^{\bullet}(OH)NHCH_3$.[5c]

EXPERIMENTAL SECTION

Materials. Isobutane, dimethyl disulfide (DMDS, Aldrich), and oxygen (Air Products) were used as received. Deuterium-labeled reagents (99.9% D) were D_2O and isobutane-d_{10}, which were purchased from Cambridge Isotope Laboratories.

***N*-Methylthioacetamide (2).** *N*-Methylthioacetamide was prepared from *N*-methylacetamide (NMAA, Aldrich), employing a standard procedure based on the Lawesson reagent,[26] and purified by silica gel column chromatography.

***N*-Methylthioacetamide-N-*d* (2b).** *N*-Methylthioacetamide (50 mg, 0.5 mmol) was stirred in 1 mL of D_2O at room temperature for 2 h, and the solvent was removed under vacuo.

***N*-(Methyl-d_3)thioacetamide (2c) and *N*-Methylthioacetamide-2,2,2-d_3 (2d).** *N*-(Methyl-d_3)thioacetamide and *N*-methylthioacetamide-2,2,2-d_3 were prepared from *N*-methylacetamide-2,2,2-d_3 and *N*-(methyl-d_3)acetamide, respectively, which in turn were synthesized according to the literature[5c] and used in the reaction with the Lawesson reagent without purification.

Methods. Neutralization−reionization mass spectra were taken on a tandem quadrupole acceleration−deceleration mass spectrometer described previously.[27] Two types of precursor ions and their deuterium labeled analogues were subjected to $^{+}$NR^{+} measurements. Protonated *N*-methylthioacetamides were generated by chemical ionization (CI). Selective protonation or deuteration at S was achieved using isobutane and isobutane-d_{10} as CI reagent gases. Typical ionization conditions were as follows: CI reagent gas pressure, 3×10^{-5} Torr; electron energy, 70−80 eV; emission current, 1 mA; ion source temperature, 210−250 °C. Cation radicals of *N*-methylthioacetamide were generated in a standard electron ionization (EI) source under the following conditions: electron energy, 70 eV; emission current, 500 μA; and temperature, 215−230 °C.

Stable precursor ions were extracted from the ion source floated at 70 V, passed through a quadrupole mass filter operated in the radio frequency-only mode and floated at 45−60 V, and accelerated with an electrostatic zoom lens maintained at an exit potential of −7180 V to obtain a total kinetic energy of 7250 eV.[27] The ions were transmitted into the neutralization collision cell floated at −7180 V, which was filled with dimethyl disulfide (DMDS) as the neutralization gas at pressures that resulted in 70% transmittance of the precursor ion beam. This corresponds to mainly (83%) single-collision conditions, according to Poisson statistics. The ions and neutrals were allowed to drift to a four-segment conduit[28] where remaining ions were deflected by the first segment floated at +250 V. The neutral flight times in the neutralization−reionization mass spectrometry ($^{+}$NR^{+}MS) measurements were 4.7−4.8 μs for the different isotopologues. The fast neutral species were reionized in the second collision cell with oxygen at the pressure that resulted in 70% transmittance of the precursor ion beam. The resulting ions were decelerated, energy filtered, and analyzed by a second quadrupole mass filter operated at unit mass resolution, while the fast neutrals were blocked by a chicane lens.[27] Typical spectra consisted of 30 accumulated repetitive scans across the full mass range and separate 200 scans of the region from m/z 70 to the survivor m/z.

Collision-induced dissociation (CID) spectra were measured on a JEOL HX-110 double-focusing mass spectrometer of forward geometry (the electrostatic sector E precedes the magnet B). Collisions with air were monitored in the first field-free region at pressures resulting in 50% transmittance of the ion beam at 10 keV. The spectra were obtained by scanning E and B simultaneously while maintaining a constant B/E ratio (B/E-linked scan).

CALCULATIONS

Standard ab initio and density functional theory calculations were performed using the Gaussian 03 suite of programs.[29] Optimized geometries of local energy minima and transition states were obtained by density functional theory calculations using Becke's hybrid functional (B3LYP)[30] and the 6-31++G-(2d,p) basis set. Harmonic frequency analysis was used to confirm the nature of stationary points as local minima (all frequencies real) or first-order saddle points (one imaginary frequency). Harmonic frequencies were calculated with B3LYP/6-31++G(2d,p), scaled by 0.963, and used to calculate zero-point vibrational energies (ZPVE). Single-point energies were calculated at several levels of theory including coupled-clusters with single, double, and perturbative triple excitations, CCSD-(T), and the 6-311G(d,p) basis set. Effective CCSD(T)/6-311++G(3df,2p) energies were obtained according to the

Table 1. Relative Energies of Thioacetamide Neutral and Ion Isomers

species/reaction	relative energy[a,b]		
	B3LYP/6-31++G(2d,p)	CCSD(T)[c]/6-311++G(3df,2p)	CCSD(T)/aug-cc-pVTZ
trans-**2** → *cis*-**2**	8.0 (−1.8)[d]	10.6 (0.7)[d]	9.7 (−0.2)[d]
trans-**2** → **3**	41	37	35
thioacetamide (**5**) → enethiol (**6**)	41	35	32
$\mathbf{5}^{+\bullet} \rightarrow \mathbf{6}^{+\bullet}$	133	147	144
trans-anti-$\mathbf{1}^+$	0	0	0
trans-syn-$\mathbf{1}^+$	7 (3)[d]	7 (3)[d]	7 (3)[d]
cis-syn-$\mathbf{1}^+$	11 (10)[d]	12 (11)[d]	12 (11)[d]
cis-anti-$\mathbf{1}^+$	11 (8)[d]	12 (9)[d]	12 (9)[d]
trans-$\mathbf{4}^+$	102 (95)[d]	87 (81)[d]	89 (82)[d]
cis-$\mathbf{4}^+$	98	85	
trans-anti-$\mathbf{1}^+$(VI)[e]		115	113
trans-syn-$\mathbf{1}^+$(VI)[e]		109	107
cis-syn-$\mathbf{1}^+$(VI)[e]		110	108
cis-anti-$\mathbf{1}^+$(VI)[e]		96	94
trans-anti-$\mathbf{1}^+ \rightarrow$ *trans*-**2** + H^+	905 (909)[f]	905 (908)[f]	905 (909)[f]
trans-syn-$\mathbf{1}^+ \rightarrow$ *trans*-**2** + H^+	898 (904)[f]	898 (903)[f]	899 (904)[f]
cis-syn-$\mathbf{1}^+ \rightarrow$ *cis*-**2** + H^+	902 (907)[f]	903 (908)[f]	903 (908)[f]
cis-anti-$\mathbf{1}^+ \rightarrow$ *cis*-**2** + H^+	902 (907)[f]	903 (908)[f]	903 (908)[f]
cis-$\mathbf{4}^+ \rightarrow$ *cis*-**2** + H^+	811 (817)[f]	828 (834)[f]	827 (832)[f]
trans-anti-$\mathbf{1}^+ \rightarrow CH_3C{=}NCH_3^+ + H_2S$	95	108	
trans-anti-$\mathbf{1}^+ \rightarrow S{=}C{=}NHCH_3^+ + CH_4$	134	143	
trans-anti-$\mathbf{1}^+ \rightarrow CH_3C{=}S^+ + CH_3NH_2$	224	226	
trans-anti-$\mathbf{1}^+ \rightarrow CH_3C(S){=}NHCH_3^{+\bullet} + H^\bullet$	359	361	
trans-anti-$\mathbf{1}^+ \rightarrow CH_3C(SH){=}NCH_3^{+\bullet} + H^\bullet$	452	471	
trans-anti-$\mathbf{1}^+ \rightarrow C(SH){=}NHCH_3^{+\bullet} + CH_3^\bullet$	436	466	
trans-anti-$\mathbf{1}^+ \rightarrow CH_3C(SH){=}NH^{+\bullet} + CH_3^\bullet$	434	469	

[a] In units of kJ mol^{-1}. [b] Including B3LYP/6-31++G(2d,p) zero-point energies and referring to 0 K. [c] Effective energies from single-point calculations according to eq 1. [d] Relative free energies at 523 K. [e] Energy difference between the cation produced by vertical ionization (VI) of the radical and the optimized cation structure. [f] Proton affinities at 298 K.

standard formula (eq 1):

$$E[(\mathrm{CCSD(T)/6\text{-}311}++\mathrm{G(3df,2p)}] \approx E[(\mathrm{CCSD(T)/6\text{-}311G(d,p)}] + E[(\mathrm{MP2/6\text{-}311}++\mathrm{G(3df,2p)}] - E[(\mathrm{MP2/6\text{-}311G(d,p)}] \quad (1)$$

In addition, CCSD(T) single-point energies were calculated using Dunning's correlation-consistent triple-ζ basis set augmented with diffuse functions on all atoms[31] (CCSD(T)/aug-cc-pVTZ).

Single-point energies of transition states were determined at the effective CCSD(T)/6-311++G(3df,2p) and the CCSD(T)/aug-cc-pVTZ levels of theory as described previously.[5a−c] Briefly, the potential energy surfaces (PES) along the rotation and dissociation coordinates were first investigated with B3LYP/6-31++G(2d,p). The dihedral angles for rotations through C_1—S and C_1—N bonds were rotated by 10° increments. The reaction pathways for S−H and N−CH_3 bond cleavages were mapped by 0.05 and 0.02 Å increments, while the remaining internal degrees of freedom were fully optimized. The points on the B3LYP PES were then treated with the effective CCSD(T)/6-311++G(3df,2p) and CCSD(T)/aug-cc-pVTZ single-point calculations to obtain corrected PES profiles. Corrected saddle points determined from polynominal fitting of these profiles were used as CCSD(T) single-point energy calculations. The energies discussed in the text are from CCSD(T)/aug-cc-pVTZ single-point calculations and include zero-point energy corrections. Data from the other calculations are given in the pertinent tables and in the Supporting Information.

The spin-unrestricted model was used for all open shell systems. Spin contamination in the UMP2, UCCSD(T) calculations was negligible for local minima. The typical value of $\langle S^2 \rangle$ operator was in the 0.75−0.77 range. For transition structures, the spin-unrestricted calculations gave $\langle S^2 \rangle$ within 1.00−0.77. Spin annihilation using Schlegel's projection method[32] (PMP2) reduced the $\langle S^2 \rangle$ values to 0.761 for transition structures and to 0.755 for local minima. Franck−Condon energies in vertical neutralization and reionization were taken as absolute differences between the CCSD(T) energies of fully optimized neutral or ion structures and those in which an electron has been added to an optimized cation structure or subtracted from an optimized neutral structure. No zero-point corrections were applied to the calculated Franck−Condon energies. In all thermochemical calculations, the rigid rotor harmonic oscillator (RRHO) model was used.

Excited electronic states were calculated using time-dependent density functional theory[33] with the B3LYP, cam-B3LYP,[34] and M06-2X[35] functionals and the aug-cc-pVTZ basis set.

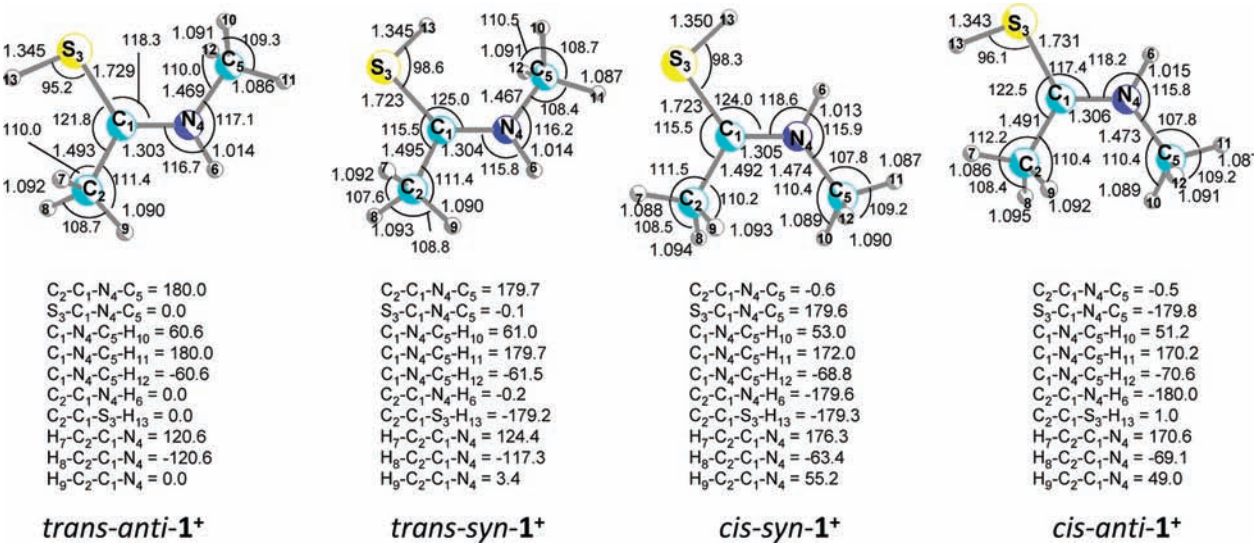

Figure 1. B3LYP/6-31++G(2d,p)-optimized structures of $\mathbf{1}^+$.

Unimolecular rate constants were calculated with Rice–Ramsperger–Kassel–Marcus (RRKM) theory[36] using Hase's program[37] that was recompiled for MS-DOS and run under Windows XP[38] or Windows 7. Vibrational state densities were obtained by a direct count of quantum states in 2 kJ mol^{-1} steps for internal energies up to 400 kJ mol^{-1} above the threshold. The rotational states were treated adiabatically, and the calculated microscopic rate constants $[k(E,J,K)]$ were Boltzmann-averaged over the thermal distribution of rotational J and K states pertaining to the ion source temperature.

RESULTS AND DISCUSSION

Radicals **1**–**1d** were generated from their cation precursors by fast collisional electron transfer. Because of the short duration of the ion-neutral collision, t = 8–10 fs,[39] the electron transfer is considered to be a near-vertical process,[40] and the radical is formed with an initial geometry, which is very similar to that of the precursor ion. Collisional electron transfer is inevitably accompanied by collision induced dissociations (CID). CID concomitant with electron transfer to $\mathbf{1}^+$ may generate neutral fragments, which are not separated from the products of electron transfer and, if formed, will appear in the $^+$NR$^+$MS spectrum after reionization. Likewise, collisional activation upon reionization can cause ion dissociations, which reflect ion, not radical, chemistry. Although CID is a minor process when CH_3SSCH_3 is used as a collision gas,[28] ion dissociations have to be identified to assess their participation in the $^+$NR$^+$MS spectra. Therefore, precursor ion generation, structures, energetics, and dissociations had to be firmly established, as discussed in the next section.

Precursor Ion Generation and Structures. Ion $\mathbf{1}^+$ was prepared by gas-phase protonation of thioacetamide (**2**). Ion $\mathbf{1a}^+$ was generated by gas-phase deuteronation of **2** with $C_4D_9^+$. Ions $\mathbf{1b}^+$, $\mathbf{1c}^+$, and $\mathbf{1d}^+$ were generated by protonation of the corresponding labeled thioacetamides with $C_4H_9^+$. Gas-phase **2** can exist as *cis* and *trans* thioamide conformers (*cis*-**2** and *trans*-**2**), which were found to have similar energies, ΔH_0(*trans*-**2** → *cis*-**2**) = 9.7 kJ mol^{-1} (Table 1), ΔG_{298}(*trans*-**2** → *cis*-**2**) = 4.0 kJ mol^{-1}. Because of its higher entropy, *cis*-**2** is slightly preferred at higher temperatures. Considering a thermal equilibrium at the ion source temperatures of 500–523 K, *cis*-**2** and *trans*-**2** are calculated to be populated in a 51:49 ratio. In addition, an enethiolimine tautomer (**3**) was obtained as a local energy minimum, which was 35 kJ mol^{-1} less stable than *trans*-**2** and was not likely to be significantly populated in the gas phase (0.03% at 523 K). For optimized structures of **2** and **3**, see Tables S1–S3 (Supporting Information).

Protonation energetics of both *cis*-**2** and *trans*-**2** favor the S atom as the likely protonation site to give aminothioketyl cations ($\mathbf{1}^+$). Four isomers of $\mathbf{1}^+$ were found as local energy minima (Figure 1). The isomers differ in the configuration of the thioamide group (*cis* or *trans*) and the conformation of the SH group (*syn* or *anti*). The most stable ion has a *trans-anti* conformation (*trans-anti*-$\mathbf{1}^+$, Figure 1) and is calculated to amount to 58% of an equilibrium mixture of ion structures at 523 K. The other conformers are *trans-syn*-$\mathbf{1}^+$ (29%), *cis-anti*-$\mathbf{1}^+$ (8%), and *cis-syn*-$\mathbf{1}^+$ (5%). In contrast, N-protonated tautomers (*trans*-$\mathbf{4}^+$ and *cis*-$\mathbf{4}^+$, Tables S4 and S5) are disfavored by 85 and 87 kJ mol^{-1}, respectively, against *trans-anti*-$\mathbf{1}^+$ and amount to <10^{-6} % at 523 K.

The 298 K proton affinities for *trans*-**2** forming *trans-anti*-$\mathbf{1}^+$ and *cis*-**2** forming *cis*-$\mathbf{4}^+$ are 909 and 832 kJ mol^{-1}, respectively, at CCSD(T)/aug-cc-pVTZ, our highest level of theory (Table 1). The large energy difference between the S- and N-protonated tautomers allows for a selective protonation at S when $C_4H_9^+$ (PA = 802 kJ mol^{-1})[41] is used as a gas-phase acid. Protonation at S in *cis*- or *trans*-**2** is 107 kJ mol^{-1} exothermic and is expected to occur at the collision rate.[42] In contrast, protonation at N is only 30 kJ mol^{-1} exothermic and therefore slower. In addition to this kinetic preference for S-protonation, a collision between *trans*-$\mathbf{4}^+$ and *cis* or *trans*-**2** would result in a highly exothermic proton transfer forming conformers $\mathbf{1}^+$ at the collisional rate. Because of the substantial number density of **2** in the CI ion source (~2 × 10^{13} molecules/cm^3), any tautomers $\mathbf{4}^+$ formed by protonation with $C_4H_9^+$ are likely to be titrated off by exothermic proton transfer to the sulfur atom in thioamide **2**.

Interconversions of *trans-anti*-$\mathbf{1}^+$ into *trans-syn*-$\mathbf{1}^+$ and *cis-syn*-$\mathbf{1}^+$ into *cis-anti*-$\mathbf{1}^+$ can occur through C_1–S bond rotations that were calculated to have low energy barriers of 42 and 30 kJ mol^{-1}, respectively. Substantially higher energy barriers were

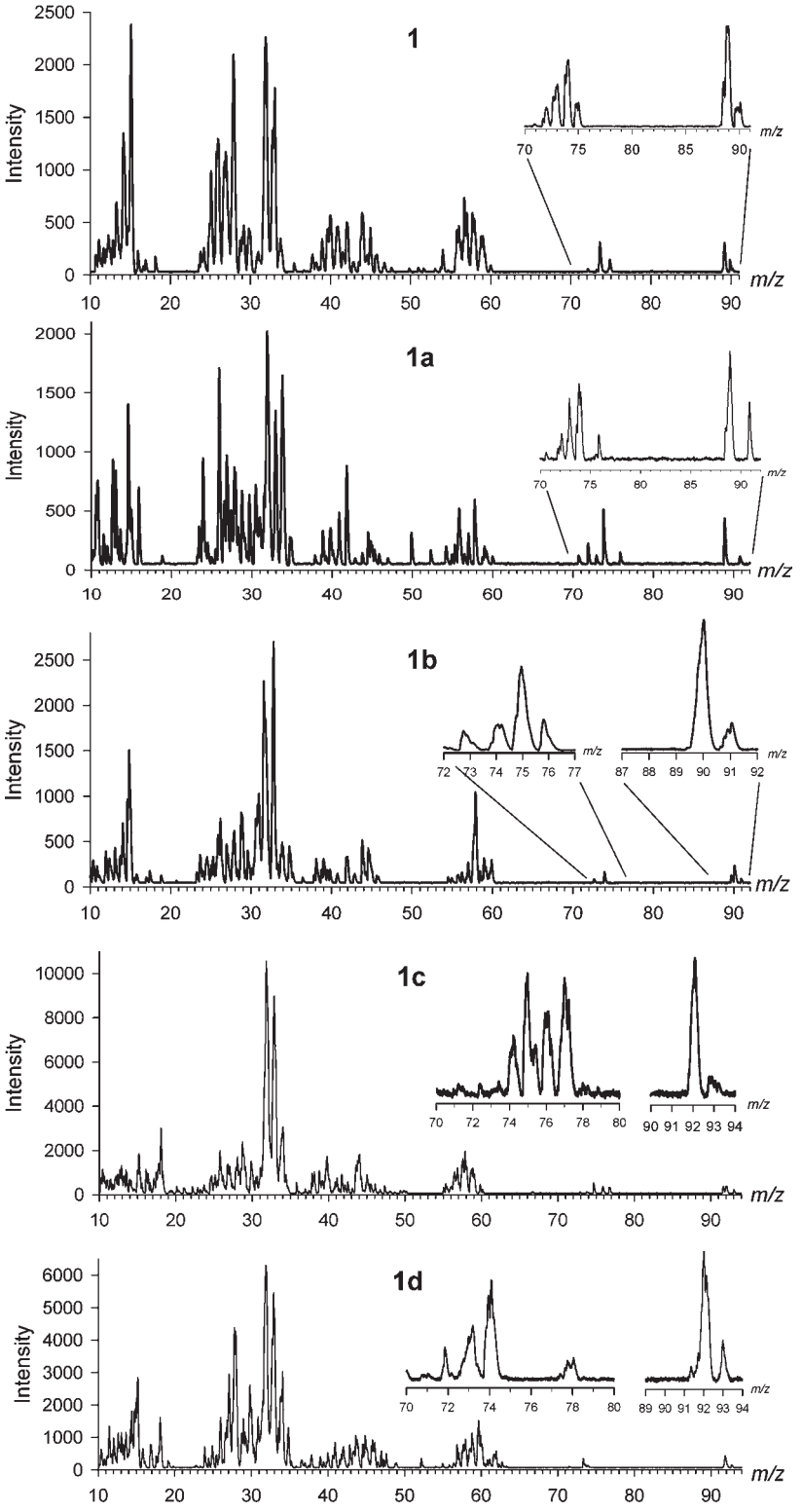

Figure 2. Neutralization (CH_3SSCH_3, 70% transmittance)−reionization (O_2, 70% transmittance) mass spectra of $\mathbf{1}^+$, $\mathbf{1a}^+$, $\mathbf{1b}^+$, $\mathbf{1c}^+$, and $\mathbf{1d}^+$. Insets show the spectra of the high mass regions that were obtained by averaging over 200 repetitive scans and are representative of the survivor and product relative abundances.

found for C_1−N bond rotations to accomplish isomerization of *trans-anti*-$\mathbf{1}^+$ to *cis-anti*-$\mathbf{1}^+$ (E_{TS} = 148 kJ mol^{-1}) and *trans-syn*-$\mathbf{1}^+$ to *cis-syn*-$\mathbf{1}^+$ (E_{TS} = 140 kJ mol^{-1}, according to CCSD(T)/aug-cc-pVTZ calculations). These TS energies indicate that *syn* and *anti* rotamers are readily interconvertible under the conditions of ion source temperature and ion residence time. However, *cis*−*trans* isomerizations are predicted to be slow, as judged by the calculated rate constants, for example, k(*cis-anti*-$\mathbf{1}^+$ →

trans-anti-$\mathbf{1}^+$) = 1.0 s^{-1} at 523 K, and are unlikely to occur on the millisecond time of ion residence in the ion source.

Precursor Ion Dissociations. Collision-induced dissociations (CID) of $\mathbf{1}^+$ and its labeled isotopomers $\mathbf{1a}^+$−$\mathbf{1d}^+$ are summarized in Figures S1 and S2 (Supporting Information). The loss of hydrogen atom is the main dissociation on CID of $\mathbf{1}^+$. Deuterium labeling in $\mathbf{1a}^+$ shows that elimination of H occurs mainly (63%) from the S−H group and less from the N−H and methyl groups (Figure S2). Thus, the main dissociation product is the *N*-methylthioacetamide cation-radical ($\mathbf{2}^{+\bullet}$). The other significant dissociations involve elimination of methylamine yielding $CH_3C{=}S^+$ (*m*/*z* 59), loss of H_2S (*m*/*z* 56), CH_3SH (*m*/*z* 42), and CH_4 (*m*/*z* 74). The elimination of methylamine is preceded by selective hydrogen atom transfer from the SH group. The hydrogen atom transfer in the elimination of hydrogen sulfide is not selective and occurs from the N−H group (57%) as well as the methyl groups, as shown by the CID spectrum of the N−D labeled ion $\mathbf{1b}^+$. The elimination of methane selectively involves the acetyl methyl group and a predominant hydrogen atom transfer from the SH group (Figure S1b).

The energetics of the main ion dissociations are summarized in Table 1. The elimination of hydrogen sulfide was calculated to be the lowest energy dissociation, requiring $\Delta H_{rxn,0}$ = 108 kJ mol^{-1} at the 0 K thermochemical threshold. The other low-energy dissociations were loss of methane and methylamine ($\Delta H_{rxn,0}$ = 143 and 226 kJ mol^{-1}, respectively). The loss of the SH hydrogen atom had a higher threshold energy, $\Delta H_{rxn,0}$ = 361 kJ mol^{-1} . The other dissociations were still more endothermic (Table 1).

It is worth noting that the dissociations of $\mathbf{1}^+$ differed significantly from those of protonated *N*-methylacetamide (NMAA).[5c] The most important difference was the abundant loss of a H atom from $\mathbf{1}^+$, which was only a minor dissociation of protonated NMAA and involved mainly hydrogen atoms from the methyl groups. The different bond dissociation energies of the S−H and O−H bonds are the likely explanation of this effect.

Formation and Dissociations of Aminothioketyl Radicals 1−1d. Collisional neutralization of $\mathbf{1}^+$ yielded a fraction of stable radicals, which were detected following reionization as survivor ions at *m*/*z* 90 in the $^+NR^+$ mass spectrum (Figure 2). The primary dissociations observed upon $^+NR^+$ were loss of $H^\bullet$ (*m*/*z* 89) and $CH_3^\bullet$ (*m*/*z* 75 and 15). The other dissociation products present in the $^+NR^+$ mass spectrum of $\mathbf{1}^+$ were formed by consecutive fragmentations of the primary dissociation products as well as by dissociations of reionized $\mathbf{1}^+$ and its fragments.

The mechanisms of the primary dissociations by loss of $H^\bullet$ and loss of $CH_3^\bullet$ were studied with $^+NR^+$ of deuterium labeled ions $\mathbf{1a}^+$, $\mathbf{1b}^+$, $\mathbf{1c}^+$, and $\mathbf{1d}^+$. $^+NR^+$ of the SD-labeled ion $\mathbf{1a}^+$ showed exclusive loss of $D^\bullet$ (*m*/*z* 89), whereas no measurable loss of $D^\bullet$ was detected in the $^+NR^+$ mass spectra of the other isotopologues of $\mathbf{1}^+$ (Figure 2). This distinguishes the loss of hydrogen atom from radical **1** from the analogous dissociation of reionized $\mathbf{1}^+$, as the CID mass spectrum of $\mathbf{1a}^+$ showed 63% loss of $D^\bullet$ and 37% loss of $H^\bullet$ (Figure S2). The combined evidence from the labeling experiments pointed to an exclusive loss of $H^\bullet$ from the SH group in radical **1**. Thus, the main primary product of dissociation of radical **1** is thioamide **2**. It is worth mentioning that the oxygen analogue of **1** behaved differently in that, although the H loss primarily occurred from the OH group, there was also H loss from the acetyl CH_3 group.[5c]

Loss of $CH_3^\bullet$ from **1** gave products that appeared at *m*/*z* 75 and 15. Deuterium labeling in the methyl groups showed a predominant loss of the N−CD_3 methyl (*m*/*z* 18 from **1c** and *m*/*z* 78 from **1d**, Figure 2), indicating that the neutral product was acetenethiolimine (**5**) (Scheme 2). The loss of the acetyl methyl group was negligible, as judged from the baseline peak intensity at *m*/*z* 78 from **1c** and *m*/*z* 75 from **1d** (Figure 2). The $^+NR^+$ mass spectra of **1a** and **1d** also showed that the loss of methyl was not accompanied by H/D exchange, which is another indication of a simple bond-cleavage radical dissociation.

Scheme 2

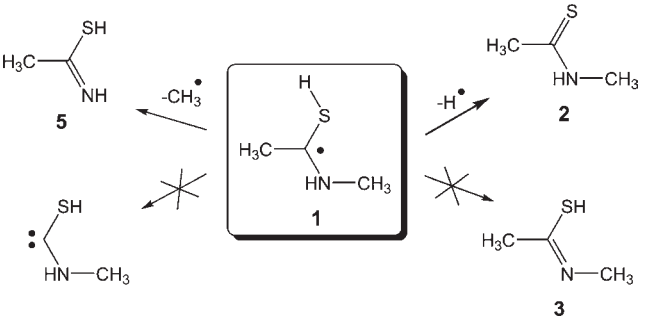

The origin of the low-mass fragments in the $^+NR^+$ mass spectrum of $\mathbf{1}^+$ was less straightforward. Some fragments can be explained by dissociations of **1** formed in high excited electronic states. Postreionization dissociations of **1** and its primary fragments **2** and **5** can also account for the formation of low-mass fragment ions. In particular, the abundant low-mass ions in the $^+NR^+$ mass spectrum of $\mathbf{1}^+$, for example, SH^+ (*m*/*z* 33) and S^+ (*m*/*z* 32), are often present as secondary fragments of sulfur-containing ions and arise by convergent dissociations induced by high-energy collisions.[43] Note that most of the dissociation products present in the $^+NR^+$ mass spectrum of $\mathbf{1}^+$ also appeared in the $^+NR^+$ mass spectrum of $\mathbf{2}^{+\bullet}$ (Figure S3a), which in turn was similar to the standard 70 eV electron−ionization mass spectrum of **2** (Figure S3b). Acetenethiolimine ($CH_3C(SH){=}NH$, **5**)[44] from loss of the *N*-methyl group from **1** is an unstable tautomer of thioacetamide (**6**) in both the neutral form (ΔH_0 (**5** → **6**) = −32 kJ mol^{-1}) and as cation radicals (ΔH_0 ($\mathbf{5}^{+\bullet}$ → $\mathbf{6}^{+\bullet}$) = −144 kJ mol^{-1}, Table 1). Although obtaining a reference $^+NR^+$ mass spectrum of $\mathbf{5}^{+\bullet}$ would be desirable, the ion instability makes $\mathbf{5}^{+\bullet}$ a difficult target. For optimized structures of **5**, $\mathbf{5}^{+\bullet}$, **6**, and $\mathbf{6}^{+\bullet}$, see Tables S6−S9.

Radical Structures and Energetics. Radical **1** was found to 5have four stable conformers, *trans-anti*-**1**, *trans-syn*-**1**, *cis-syn*-**1**, and *cis-anti*-**1** (Figure 3), that were analogous to those found for ion $\mathbf{1}^+$. Yet another low-energy conformer, *trans-anti*-**1′**, was found as a rotamer of *trans-anti*-**1** from B3LYP/6-31++G(2d,p) analysis of the potential energy surface (PES) for C_1−S rotations. Vertical transitions between the pertinent ion and radical conformers were associated with Franck−Condon energies of 51, 56, 59, and 54 kJ mol^{-1} for *trans-anti*-$\mathbf{1}^+$ → *trans-anti*-**1**, *trans-syn*-$\mathbf{1}^+$ → *trans-syn*-**1**, *cis-syn*-$\mathbf{1}^+$ → *cis-syn*-**1**, and *cis-anti*-$\mathbf{1}^+$ → *cis-anti*-**1** transitions, respectively, from effective CCSD(T)/6-311++G(3df,2p). These contribute to vibrational excitation of the radical **1** conformers when formed by collisional electron transfer, as discussed later.

The radical **1** conformers had relative energies within 6 kJ mol^{-1} (Table 2). Interconversions of radical **1** conformers occurred through a combination of C_1−S and C_1−N bond rotations. The transition states for rotations about the C_1−S and C_1−N bonds in **1** had low energies. For example, rotation about the C_1−N bond in *cis-syn*-**1** had an energy barrier of 25 kJ mol^{-1}

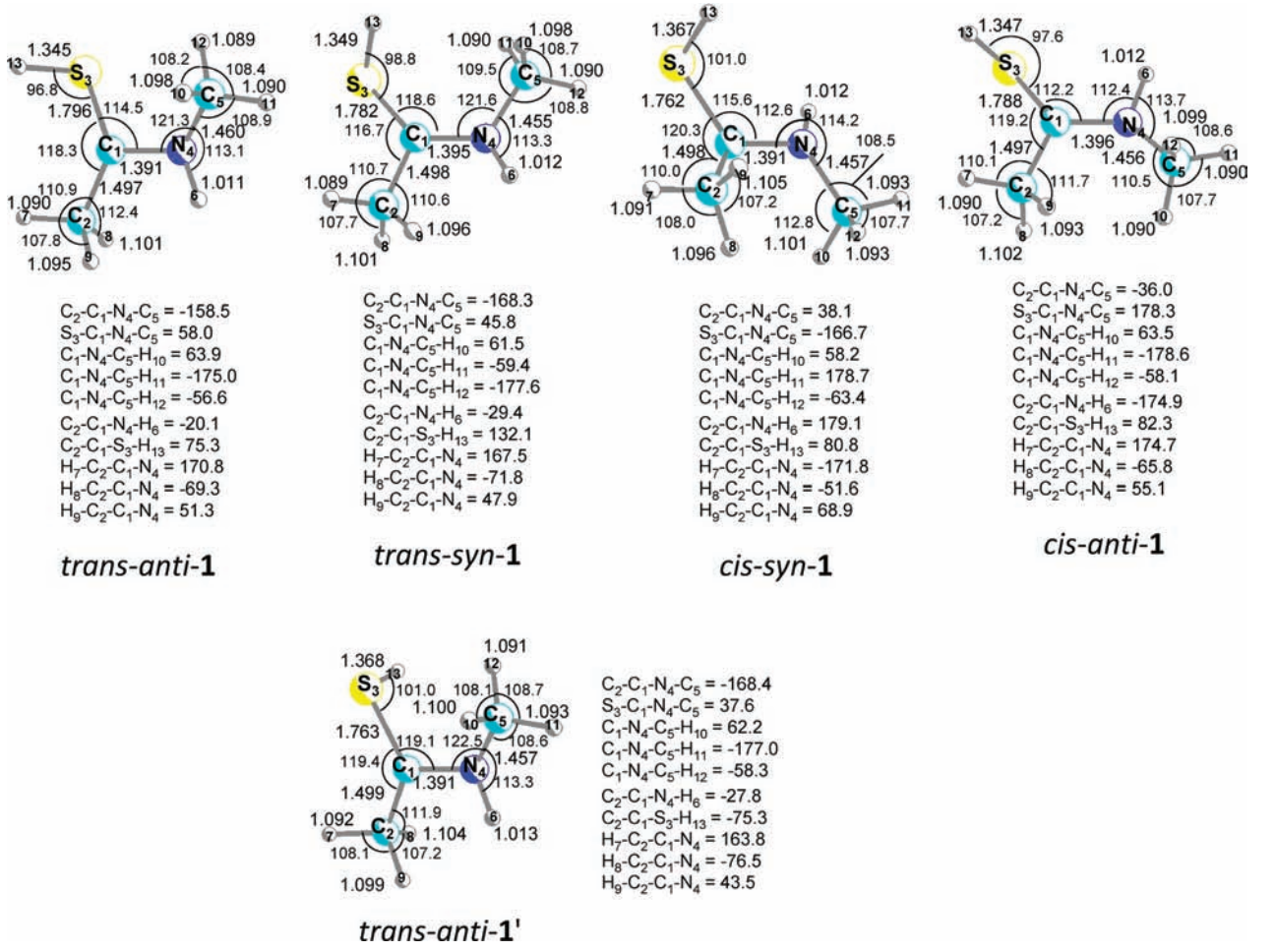

Figure 3. B3LYP/6-31++G(2d,p)-optimized structures of radical isomers.

to be compared to an analogous barrier in the ion (128 kJ mol^{-1}). Hence, interconversion of *cis* and *trans* as well as *syn* and *anti* conformers was possible in radical **1** and could proceed through multiple pathways of coupled rotations. It is worth noting that the energy barriers for both C_1-S and C_1-N bond rotations in radical **1** were somewhat higher than those calculated for the 1-hydroxy-1-(*N*-methyl)aminoethyl radical.[5c]

Radical Dissociation Energies. Potential energy surface calculations were performed to elucidate the cleavages of S−H and N−CH_3 bonds, which were the primary unimolecular dissociations observed upon electron transfer. Dissociations of the S−H bonds in *cis-syn*-**1** and *cis-anti*-**1** converged to the same transition state (**TS1**) (Figure 4), which was 98 kJ mol^{-1} above *cis-syn*-**1** (Table 2). The transition states for S−H bond cleavages in *trans-anti*-**1**, *trans-anti*-**1**′ (**TS2**), and *trans-syn*-**1** (**TS3**) were both at 93 kJ mol^{-1} above the respective reactants, but differed in the acetyl CH_3 conformations (Figure 4). A common feature of **TS1**−**TS3** was that they were late transition states in which the thioacetamide C_2,C_1S,N-framework was nearly planar and the departing hydrogen atom was in the S−C_1−N plane. This was consistent with the S−H bond dissociation energies in the aminothioketyl radicals that were very close to the pertinent TS energies (Table 2). This indicates that H-atom additions to *cis* and *trans* thioamides should have negligible activation energies.

The PES profiles along the S−H coordinates from B3LYP and CCSD(T) calculations showed different shapes (Figure S4a). The B3LYP-PES from *cis-syn*-**1** showed an apparent saddle point (**TS1**) with a correct curvature at a nuclear separation of *d*(S−H) = 2.16 Å, but the potential energy further increased at greater atom separations. The CCSD(T) PES showed a more pronounced TS at *d*(S−H) = 2.05−2.06 Å (Figure S4a). The differences were more dramatic for S−H bond cleavage in *trans-syn*-**1** where, according to the PES curvature, apparent **TS2** and **TS3** occurred at *d*(S−H) = 2.34−2.35 Å by B3LYP, while CCSD(T) gave saddle points at *d*(S−H) = 2.10−2.20 Å (Figure S4b).

Two nearly identical transition states were located for N−CH_3 bond cleavages in *cis-syn*-**1** (**TS4**) and *cis-anti*-**1** (**TS5**) (Figure 4), which differed only in the torsional angles of the departing methyl groups and had virtually identical energies, $E_{TS4} \approx E_{TS5}$ = 109 kJ mol^{-1} above *cis-syn*-**1**. Dissociations of the N−H and CH_3−C bonds in *cis*-**1** were also studied, but showed higher TS energies, for example, E_{TS8} = 142 kJ mol^{-1} and E_{TS9} = 217 kJ mol^{-1}, respectively. Cleavages of the N−CH_3 bonds in *trans*-**1** isomers had transition states at 110 and 113 kJ mol^{-1} for **TS6** and **TS7**, respectively. The relative and TS energies for all dissociations and isomerizations of **1** are plotted in a potential energy diagram (Figure 5). This shows that the energetically most favorable dissociation is cleavage of the S−H bond through **TS2** or **TS3**. The loss of *N*-methyl required somewhat higher TS energies, the lowest of which was in **TS4** and **TS5**. The TS energies for the *syn*−*anti* and *cis*−*trans* rotations were much lower than those for

Table 2. Relative Energies of Thioacetamide Radicals

species/reaction	relative energy[a,b]		
	B3LYP/6-31++G(2d,p)	CCSD(T)[c]/6-311++G(3df,2p)	CCSD(T)/aug-cc-pVTZ
cis-syn-**1**	0	0	0
trans-anti-**1**	6	5	4
trans-anti-**1**′	1	0	0
trans-syn-**1**	6	5	4
cis-anti-**1**	6	6	5
cis-syn-**1** (VN)[d]		59	
trans-anti-**1** (VN)[d]		56	
trans-syn-**1** (VN)[d]		56	
cis-anti-**1** (VN)[d]		60	
cis-syn-**1** → *cis*-**2** + H$^\bullet$		94	101
trans-anti-**1**′ → *trans*-**2** + H$^\bullet$		84	91
cis-anti-**1** → *anti*-**4** + $CH_3^\bullet$		51	51
trans-anti-**1**′ → *syn*-**4** + $CH_3^\bullet$		57	58
cis-syn-**1** → *cis*-**3** + H$^\bullet$		130	
cis-syn-**1** → C(SH)−$NHCH_3$ + $CH_3^\bullet$		201	
TS1	87 (2.157)[e]	96 (2.065)[e]	98 (2.053)[e]
TS2	90 (2.347)[e]	89 (2.123)[e]	93 (2.172)[e]
TS3	91 (2.341)[e]	89 (2.111)[e]	93 (2.196)[e]
TS4	101 (2.098)[e]	113 (2.061)[e]	109 (2.064)[e]
TS5	101 (2.097)[e]	113 (2.063)[e]	109 (2.076)[e]
TS6	102 (2.087)[e]	114 (2.059)[e]	110 (2.060)[e]
TS7	100 (2.087)[e]	116 (2.060)[e]	113 (2.062)[e]
TS8	146 (1.936)[e]	142 (1.978)[e]	
TS9	205 (2.623)[e]	216 (2.514)[e]	217 (2.552)[e]

[a] In units of kJ mol^{-1}. [b] Including B3LYP/6-31++G(2d,p) zero-point energies and referring to 0 K. [c] Effective energies from single-point calculations according to eq 1. [d] Energy difference between the vertically neutralized radical and the optimized structure. [e] Transition state bond lengths in Ångstrøms.

the dissociations. This indicated that the various conformers of **1** can readily interconvert before undergoing dissociation.

The PES we obtained for **1** was substantially different from that reported previously for the 1-hydroxy-1-(*N*-methyl)aminoethyl radical,[5c] which showed very small differences between transition state energies for O−H and N−CH_3 dissociations that were kinetically competitive.

A particular aspect of the thioamide group is the very low barrier for H-atom addition to the sulfur atom. This indicates that thioamides can be efficient scavengers of hydrogen atoms in larger systems such as thioxopeptide radicals that can affect radical-induced backbone dissociations and peptide sequencing.

Dissociation Kinetics of 1. The kinetics of S−H and N−CH_3 bond dissociations of **1** were investigated with RRKM calculations on the effective CCSD(T)/6-311++G(3df,2p) and CCSD(T)/aug-cc-pVTZ potential energy surfaces and using B3LYP/6-31++G(2d,p) zero-point corrections, harmonic frequencies, and moments of inertia. Because of the presumably fast interconversion of **1** rotamers over the very low rotation barriers, the most stable *cis-syn*-**1** radical was selected as a common reactant. To assess isotope effects, unimolecular rate constants were also calculated for dissociations of all experimentally studied isotopologues of *cis-syn*-**1** (Figure S5, Supporting Information). The rate constants for loss of H and CH_3 from *cis-syn*-**1**, which are based on the CCSD(T)/aug-cc-pVTZ energies, are shown in Figure 6 as log *k* plotted against the radical internal energy. The loss of H is favored at internal energies up to 232 kJ mol^{-1} where the log *k* curves cross. This result is in general agreement with the $^{+}NR^{+}$ mass spectrum of $\mathbf{1}^+$, which showed a more abundant peak for loss of H (*m*/*z* 89) than for loss of CH_3 (*m*/*z* 75). The neutral dissociations and fragment ion formation can be expressed by convoluting the RRKM rate constants $k(E)$ with an internal energy distribution function $P(E)$ (eqs 2 and 3), where [M], [M − H], and [M − CH_3] are the ion relative intensities, *t* is the time for dissociation (4.8 μs), and σ_M, σ_{M-H}, and σ_{M-CH3} are the pertinent ionization cross sections.

$$\frac{[M-H]}{[M]} = \frac{\sigma_{M-H}\int_{E_{TS}}^{\infty} P(E)\frac{k_H(E)}{k_H(E)+k_{CH_3}(E)}\{1-e^{-[k_H(E)+k_{CH_3}(E)]t}\}\,dE}{\sigma_M\int_{E_{TS}}^{\infty} P(E)e^{-[k_H(E)+k_{CH_3}(E)]t}\,dE} \quad (2)$$

$$\frac{[M-H]}{[M-CH_3]} = \frac{\sigma_{M-H}\int_{E_{TS}}^{\infty}\frac{k_H(E)}{k_H(E)+k_{CH_3}(E)}P(E)\{1-e^{-[k_H(E)+k_{CH_3}(E)]t}\}\,dE}{\sigma_{M-CH_3}\int_{E_{TS}}^{\infty}\frac{k_{CH_3}(E)}{k_H(E)+k_{CH_3}(E)}P(E)\{1-e^{-[k_H(E)+k_{CH_3}(E)]t}\}\,dE} \quad (3)$$

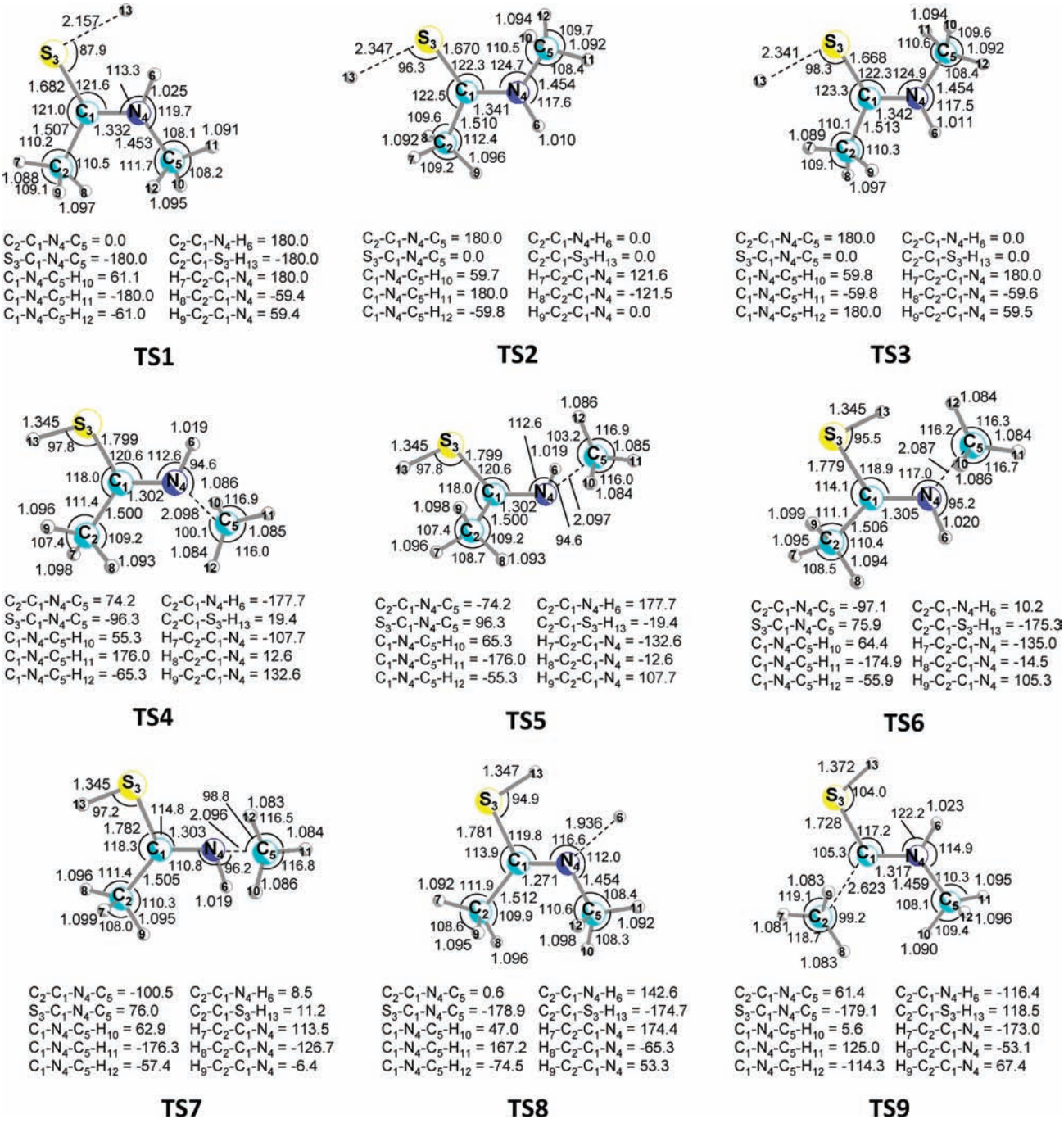

Figure 4. B3LYP/6-31++G(2d,p)-optimized structures of **TS1**−**TS9**.

The σ_{M-H}/σ_M and $\sigma_{M-H}/\sigma_{M-CH3}$ relative ionization cross sections were estimated from the atomic increments of Fitch and Sauter[45] as 0.97 and 1.24. The distribution function $P(E)$ was modeled by eq 4, where E_0 is an onset energy and W is a width parameter.[46]

$$P(E) = \frac{4(E - E_0)}{W^2} e^{-2(E - E_0)/W} \quad P(E) = 0 \text{ for } E \le E_0 \quad (4)$$

Parameters E_0 and W were least-squares fitted into eq 2 to reproduce the experimental [M − H]/M ratios from **1** and **1d** (0.157 and 0.169, respectively), and the [M − D]/M ratio from **1a** (0.243). A fit with E_0 = 79 kJ mol^{-1} and W = 95 kJ mol^{-1} (Figure 6) reproduced the experimental ion intensity ratios within ±0.006 (4%) root-mean square deviation. The distribution has a maximum at E_{max} = 127 kJ mol^{-1} and a mean at $\langle E \rangle$ = 174 kJ mol^{-1} (Figure 6). The mean energy of **1** formed by electron transfer can be composed of terms due to the rovibrational enthalpy of **2** (ΔH_{rovib} = 32 kJ mol^{-1} at 523 K), a fraction of protonation exothermicity (ΔPA = 909 − 802 = 107 kJ mol^{-1}), and the Franck−Condon energy upon vertical electron transfer (56−61 kJ mol^{-1}). The partitioning of the protonation exothermicity between $\mathbf{1}^+$ and isobutene is a priori unknown, but it can be estimated as ranging from 80% of ΔPA[47] deposited in $\mathbf{1}^+$ (86 kJ mol^{-1}) down to equipartition among the internal degrees

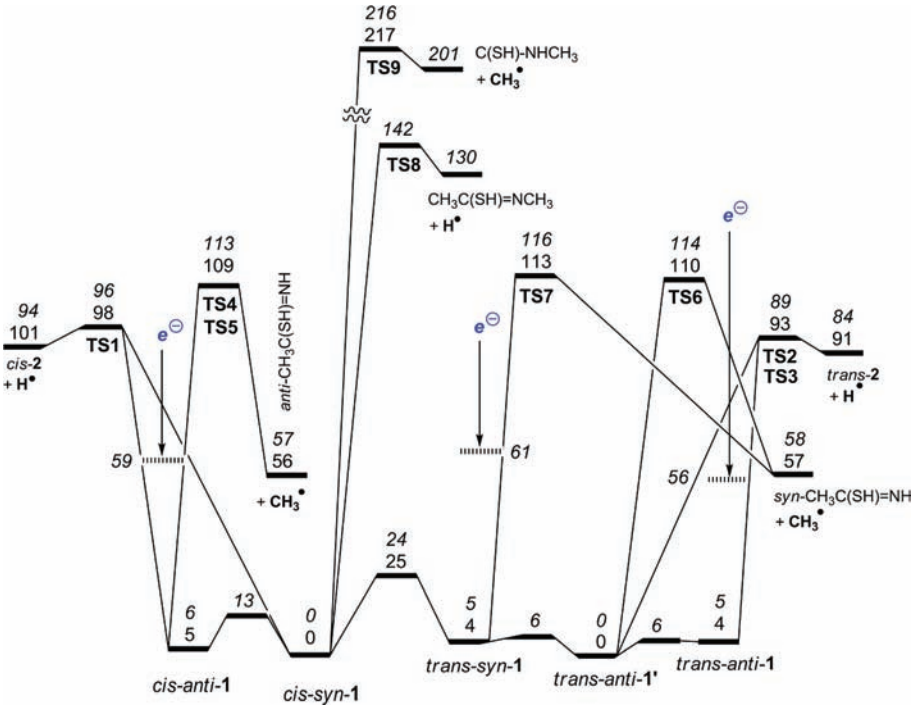

Figure 5. The potential energy diagram for dissociations of **1** from CCSD(T)/aug-cc-pVTZ (roman characters) and 6-311++G(3df,2p) (italics) single-point energy calculations and B3LYP/6-31++G(2d,p) zero-point corrections.

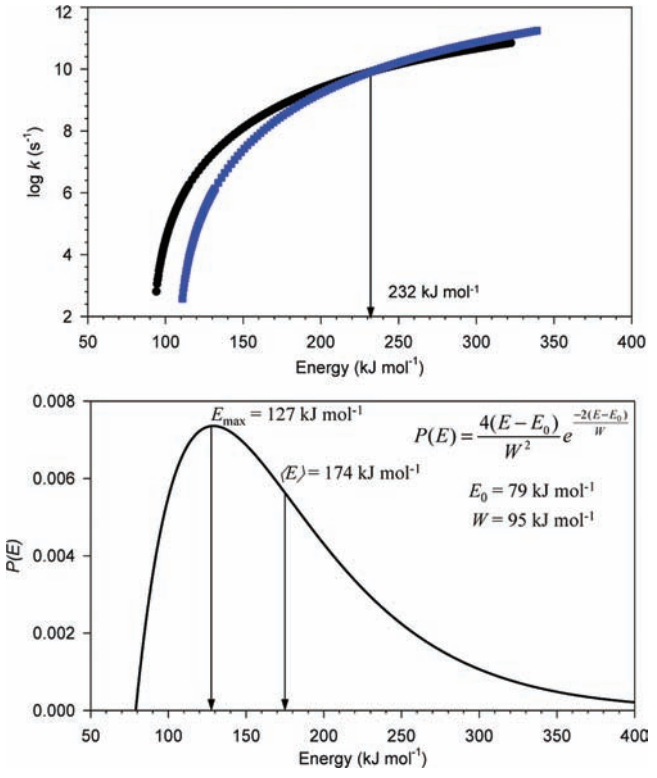

Figure 6. Top panel: RRKM unimolecular rate constants for dissociations of **1**. Black ●, S−H bond cleavage; blue ■, N−CH_3 bond cleavage. Bottom panel: Internal energy distribution in **1**.

of freedom of both products to give 54 kJ mol^{-1} in $\mathbf{1}^+$. From these terms, one obtains the mean energy E_{int} ranging from 142 to 179 kJ mol^{-1}. This range of internal energies is very well covered by the fitted $P(E)$ function, which has $\langle E \rangle$ = 174 kJ mol^{-1} (Figure 6).

Equation 3 gives the calculated [M − H]/[M − CH_3] ratio as 2.9, which is somewhat lower than the experimental value of 5.2. The latter value matches the RRKM-calculated [M − H]/[M − CH_3] ratio at E_{int} = 150 kJ mol^{-1}, which is between the E_{max} and $\langle E \rangle$ of the fitted $P(E)$ distribution. The calculated primary kinetic isotope effect for the loss of H from **1** and the loss of D from **1a** ranges from k_H/k_D = 3.5 to 2.2 in the energy interval between E_{max} and $\langle E \rangle$. The internal energy distribution function in Figure 6 predicts that ca. 10% of **1** does not dissociate on the 4.8 μs time scale of the experiment. The actual relative abundance of $\mathbf{1}^+$ in the $^+NR^+$ mass spectrum is lower. In part this is due to postreionization dissociations of $\mathbf{1}^+$. Another factor may be dissociations occurring from excited electronic states of **1** that are accessed by electron transfer at keV collision energies. Excited-state dissociations can also account for the formation of low-mass fragments seen in the $^+NR^+$ mass spectra. TD-DFT calculations with B3LYP, cam-B3LYP, and M06-2X functionals indicated that the low excited states of vertically formed **1** were represented by combinations of σ^* orbitals (Figure S6, Supporting Information). The first excited (A′) state had a large component from the σ^*(N−H) orbital. If formed, the A′ state would presumably lead to N−H bond cleavage, which, however, was not observed experimentally. The next excited state (B′) had a large component from the σ^*(S−H) orbital. If formed, the B′ state would presumably lead to S−H bond cleavage and thus enhance the experimentally observed formation of thioacetamide above that calculated for ground-state dissociations.

■ CONCLUSIONS

This experimental and computational study of aminothioketyl radical **1** showed a substantial fraction of stable radicals formed

by fast electron transfer. The main unimolecular dissociation of **1** was S−H bond cleavage resulting in the specific loss of the thiol hydrogen atom. At internal energies >232 kJ mol^{-1}, cleavage of the N−CH_3 bond became faster, leading to loss of the amide methyl group. The results obtained for **1** indicated that substitution of sulfur for amide oxygen in this simple model system induced substantial changes in the dissociation mechanisms and kinetics. We expect similar effects to operate in electron-based dissociations of thioamide groups in thiooxo analogues of gas-phase peptides. Experimental and computational studies of thioxopeptides and effects on cation-radical dissociations of thioamide substitution are underway in this laboratory.

■ ASSOCIATED CONTENT

Supporting Information. Complete refs 5d and 29, Tables S1−S42 with optimized structures, total and zero-point energies, and Figures S1−S6. This material is available free of charge via the Internet at http://pubs.acs.org.

■ AUTHOR INFORMATION

Corresponding Author
turecek@chem.washington.edu

Present Addresses
[†]Institute of Organic Chemistry, Polish Academy of Sciences, Warsaw, Poland.

■ ACKNOWLEDGMENT

Support of this research by the National Science Foundation (Grants CHE-0750048 for experiments and CHE-0342956 for computations) is gratefully acknowledged. The Department of Chemistry Computational Center has been supported jointly by the NSF and University of Washington. We thank Dr. Martin Sadilek for technical assistance with mass spectra measurements. The JEOL HX-110 mass spectrometer was a generous donation from the former Seattle Biomembrane Institute by courtesy of Prof. S. Hakomori.

■ REFERENCES

(1) von Sonntag, C. *Adv. Quantum Chem.* **2007**, *52*, 5–20.
(2) (a) Besic, E. *J. Mol. Struct.* **2009**, *917*, 71–75. (b) Eriksson, L. A.; Kryachko, E. S.; Nguyen, M. T. *Int. J. Quantum Chem.* **2004**, *99*, 841–853. (c) Gomzi, V.; Herak, J. N. *J. Mol. Struct. (THEOCHEM)* **2003**, *629*, 71–76.
(3) (a) Zubarev, R. A.; Kelleher, N. L.; McLafferty, F. W. *J. Am. Chem. Soc.* **1998**, *120*, 3265–3266. (b) Zubarev, R. A.; Horn, D. M.; Fridriksson, E. K.; Kelleher, N. L.; Lewis, M. A.; Carpenter, B. A.; McLafferty, F. W. *Anal. Chem.* **2000**, *72*, 563–573. (c) Chung, T. W.; Turecek, F. *Int. J. Mass Spectrom.* **2011**, *301*, 55–61.
(4) (a) Zubarev, R. A. *Mass Spectrom. Rev.* **2003**, *22*, 57–77. (b) Hakånsson, K.; Klassen, J. S. *Electrospray and MALDI Mass Spectrometry*, 2nd ed.; Wiley: New York, 2010; pp 571−630.
(5) (a) Syrstad, E. A.; Tureček, F. *J. Phys. Chem. A* **2001**, *105*, 11144–11155. (b) Tam, F.; Syrstad, E. A.; Chen, X.; Tureček, F. *Eur. J. Mass Spectrom.* **2004**, *10*, 869–879. (c) Syrstad, E. A.; Stephens, D. D.; Tureček, F. *J. Phys. Chem. A* **2003**, *107*, 115–126. (d) Al-Khalili, A.; et al. *J. Chem. Phys.* **2004**, *121*, 5700–5708.
(6) (a) Breuker, K.; Oh, H. B.; Horn, D. M.; Cerda, B. A.; McLafferty, F. W. *J. Am. Chem. Soc.* **2002**, *124*, 6407–6420. (b) Breuker, K.; Oh, H. B.; Lin, C.; Carpenter, B. K.; McLafferty, F. W. *Proc. Natl. Acad. Sci. U.S.A.* **2002**, *99*, 15863–15868. (c) Robinson, E. W.; Leib, R. D.; Williams, E. R. *J. Am. Soc. Mass Spectrom.* **2006**, *17*, 1469.
(7) (a) Tureček, F. *J. Am. Chem. Soc.* **2003**, *125*, 5954–5963. (b) Skurski, P.; Sobczyk, M.; Jakowski, J.; Simons, J. *Int. J. Mass Spectrom.* **2007**, *265*, 197–212.
(8) Scheibye, S.; Pedersen, B. S.; Lawesson, S.-O. *Bull. Soc. Chim. Belg.* **1978**, *87*, 229–238.
(9) Clausen, K.; Thorsen, M.; Lawesson, S.-O. *Tetrahedron* **1981**, *37*, 3635–3639.
(10) Ozturk, T.; Ertas, E.; Mert, O. *Chem. Rev.* **2007**, *107*, 5210–5278.
(11) Ilankumaran, P.; Ramesha, A. R.; Chandrasekaran, S. *Tetrahedron Lett.* **1995**, *36*, 8311–8314.
(12) Lajoie, G.; Lepine, F.; Maziak, L.; Belleau, B. *Tetrahedron Lett.* **1983**, *24*, 3815–3818.
(13) Yokoyama, M.; Hasegawa, Y.; Hatanaka, H.; Kawazoe, Y.; Imamoto, T. *Synthesis* **1984**, *84*, 827–829.
(14) Goel, O. P.; Krolls, U. *Synthesis* **1987**, *87*, 162–164.
(15) Hollosi, M.; Maler, Z.; Zewdu, M.; Ruff, F.; Kajtar, M.; Kover, K. E. *Tetrahedron* **1988**, *44*, 195–202.
(16) Bardi, R.; Piazessi, A. M.; Toniolo, C.; Jensen, O. E.; Omar, R. S.; Senning, A. *Biopolymers* **1988**, *27*, 747–761.
(17) Varughese, K. I.; Przybylska, M.; Sestanj, K.; Bellini, F.; Humber, L. C. *Can. J. Chem.* **1983**, *61*, 2137–2140.
(18) Walther, W.; Voss, J. In *The Chemistry of Amides*; Zabicky, J., Ed.; Wiley-Interscience: New York, 1970.
(19) Bondi, A. *J. Phys. Chem.* **1964**, *68*, 441–451.
(20) LaCour, T. F. M. *Int. J. Pept. Protein Res.* **1987**, *30*, 564–571.
(21) Lee, H.-J.; Kim, J. H.; Jung, H. J.; Kim, K.-Y.; Kim, E.-J.; Choi, Y.-S.; Yoon, C.-J. *J. Comput. Chem.* **2004**, *25*, 169–178 and references therein.
(22) Seebach, D.; Ko, S. Y.; Kessler, H.; Kock, M.; Reggelin, M.; Schmieder, P.; Walkinshaw, D.; Boelsterli, J. J.; Bevec, D. *Helv. Chim. Acta* **1991**, *74*, 1953–1990.
(23) Kessler, H.; Geyer, A.; Matter, H.; Köck, M. *Int. J. Pept. Protein Res.* **1992**, *40*, 25–40.
(24) (a) Williams, B. W.; Porter, R. F. *J. Chem. Phys.* **1980**, *73*, 5598–5604. (b) Danis, P. O.; Wesdemiotis, C.; McLafferty, F. W. *J. Am. Chem. Soc.* **1983**, *105*, 7454–7455. (c) Burgers, P. J.; Holmes, J. L.; Mommers, A. A.; Terlouw, J. K. *Chem. Phys. Lett.* **1983**, *102*, 1–3.
(25) For reviews of the technique, see: (a) Turecek, F. *Top. Curr. Chem.* **2003**, *225*, 77–129. (b) Zagorevskii, D. V.; Holmes, J. L. *Mass Spectrom. Rev.* **1999**, *18*, 87–118. (c) Schalley, C. A.; Hornung, G.; Schroder, D.; Schwarz, H. *Chem. Soc. Rev.* **1998**, *27*, 91–104.
(26) Thomsen, I.; Clausen, K.; Scheibye, S.; Lawesson, S.-O. *Org. Synth.* **1984**, *62*, 158–163.
(27) Tureček, F.; Gu, M.; Shaffer, S. A. *J. Am. Soc. Mass Spectrom.* **1992**, *3*, 493–501.
(28) Tureček, F. *Org. Mass Spectrom* **1992**, *27*, 1087–1097.
(29) Frisch, M. J.; et al. *Gaussian 03*; Gaussian, Inc.: Wallingford, CT, 2004.
(30) (a) Becke, A. D. *J. Chem. Phys.* **1993**, *98*, 1372–1377. (b) Stephens, P. J.; Devlin, F. J.; Chabalowski, C. F.; Frisch, M. J. *J. Phys. Chem.* **1994**, *98*, 11623–11627.
(31) Dunning, T. H., Jr. *J. Chem. Phys.* **1989**, *90*, 1007–1023.
(32) (a) Schlegel, H. B. *J. Chem. Phys.* **1986**, *84*, 4530–4534. (b) Mayer, I. *Adv. Quantum Chem.* **1980**, *12*, 189–262.
(33) Furche, F.; Ahlrichs, R. *J. Chem. Phys.* **2002**, *117*, 7433–7447.
(34) Yanai, T.; Tew, D. P.; Handy, N. C. *Chem. Phys. Lett.* **2004**, *393*, 51–57.
(35) Zhao, Y.; Truhlar, D. G. *Theor. Chem. Acc.* **2008**, *120*, 215–241.
(36) Gilbert, R. G.; Smith, S. C. *Theory of Unimolecular and Recombination Reactions*; Blackwell Scientific Publications: Oxford, 1990.
(37) Zhu, L.; Hase, W. L. *Quantum Chemistry Program Exchange*; Indiana University: Bloomington, IN, 1994; Program QCPE 644.
(38) Frank, A. J.; Sadilek, M.; Ferrier, J. G.; Tureček, F. *J. Am. Chem. Soc.* **1997**, *119*, 12343–12353.

(39) This follows from the precursor ion velocity (v = 1.247 × 10^7 cm s^{-1} at 7250 eV) and the typical cross section for electron transfer ($\sigma \approx 10^{-14}$ cm^2), according to the formula $t \approx (2/v)(\sigma/\pi)^{1/2}$.
(40) Holmes, J. L. *Mass Spectrom. Rev.* **1989**, *8*, 513–539.
(41) Traeger, J. C. *Rapid Commun. Mass Spectrom.* **1996**, *10*, 119–122.
(42) Böhme, D. K.; Mackay, G. I.; Schiff, H. I. *J. Chem. Phys.* **1980**, *73*, 4976–4986.
(43) No, M.-H.; Turecek, F. *J. Mass Spectrom.* **1997**, *32*, 838–845.
(44) Lapinski, L.; Rostkowska, H.; Khvorostov, A.; Nowak, M. J. *Phys. Chem. Chem. Phys.* **2003**, *5*, 1524–1529.
(45) Fitch, W. L.; Sauter, A. D. *Anal. Chem.* **1983**, *55*, 832–835.
(46) (a) Wolken, J. K.; Tureček, F. *J. Phys. Chem. A* **1999**, *103*, 6268–6281. (b) Tureček, F. *Int. J. Mass Spectrom.* **2003**, *227*, 327–338.
(47) Uggerud, E. *Adv. Mass Spectrom.* **1995**, *13*, 53–70.